ELSEVIER

Journal of Pharmaceutical and Biomedical Analysis
14 (1996) 749–753

JOURNAL OF
PHARMACEUTICAL
AND BIOMEDICAL
ANALYSIS

Pharmacokinetics of osthole in rat plasma using high-performance liquid chromatography

T.H. Tsai[a,b,*], T.R. Tsai[c], C.C. Chen[a], C.F. Chen[a,d]

[a]*Department of Pharmacology, National Research Institute of Chinese Medicine, Shih-Pai, Taipei 11221, Taiwan*
[b]*Institute of Traditional Medicine, National Yang-Ming University, Shih-Pai, Taipei 11221, Taiwan*
[c]*Graduate Institute of Pharmaceutical Sciences, Kaohsiung Medical College, Kaohsiung 807, Taiwan*
[d]*Department of Pharmacology, National Yang-Ming University, Shih-Pai, Taipei 11221, Taiwan*

Received for review 17 August 1995; revised manuscript received 25 September 1995

Abstract

A simple high-performance liquid chromatographic method was developed to study the pharmacokinetics of osthole in rat plasma. After addition of an internal standard (paeonol), plasma was deproteinized by acetonitrile for sample clean-up. The drugs were separated on a reversed-phase column and detected by UV absorption at 323 nm. Acetonitrile–water–diethylamine (50:50:0.1, v/v/v) (pH 3.0, adjusted with orthophosphoric acid) was used as the mobile phase. It was applied to the pharmacokinetic study of osthole in rats after a dose of 10 mg kg^{-1} by intravenous administration. A biphasic phenomenon with a rapid distribution followed by a slower elimination phase was observed from the plasma concentration–time curve.

Keywords: Angelica pubescens; Osthole; Pharmacokinetics; Photodiode-array detection

1. Introduction

Osthole, a chemical principle isolated from the root of *Angelica pubescens* Maxim (Chinese name: Du Huo) [1], has been used in oriental countries over hundreds of years as a remedy for arthritis, lumbago, edema, headache, common cold, thrombosis, stasis of blood [2] and anti-inflammatory and analgesic activities [3]. It has been reported that osthole inhibits platelet aggregation [4] and release reaction through the suppression of thromboxane formation and phosphoinositide breakdown [5]. Osthole also exhibits vasorelaxant action by elevation of cGMP levels of vascular smooth muscle and inhibition of calcium influx [6]. Teng et al. [7] concluded that osthole exerts a non-specific relaxant effect on the trachealis by inhibiting the cAMP and cGMP phosphodiesterases. However, the determination of osthole in plasma and its pharmacokinetic properties have not been studied. In this work, a high-performance liquid chromatographic (HPLC) method with photodiode-array and UV detection was de-

* Corresponding author, at Department of Pharmacology, National Research Institute of Chinese Medicine, Shih-Pai, Taipei 11221, Taiwan. Fax: 886-2-8201856.

SSDI 0731-7085(95)01692-9

veloped to determine the concentration of osthole in rat plasma and its related pharmacokinetic profile.

2. Experimental

2.1. Chemicals and reagents

Osthole (Fig. 1) was extracted from the roots of *Angelica pubescens*. The dried root (10 kg) was extracted with hot methanol. After evaporation of the solvent, a brown, viscous residue (4.2 kg) was obtained. The residue was partitioned between water and chloroform, ethyl acetate and *n*-butanol in sequence to give a chloroform extract (692 g), ethyl acetate extract (60.6 g) and *n*-butanol extract (325 g), respectively. The chloroform extract was column chromatographed on silica gel and eluted with gradients of chloroform and methanol to afford eight fractions. Fraction 2 was rechromatographed on a silica gel column with *n*-hexane–ethyl acetate (20:1) as eluent to give 13 fractions. Osthole (3.2 g) was obtained from fractions 10 and 11 [4]. The identification and purity (98%) of osthole were compared with an authentic compound by ^{13}C NMR spectrometry (Bruker, Karlsruhe, Germany) and HPLC with photodiode-array detection (Fig. 2). Acetonitrile and orthophosphoric acid (85%) were obtained from Merck (Darmstadt, Germany). Triply deionized water (Millipore, Bedford, MA, USA) was used for all preparations.

2.2. Apparatus and chromatography

The HPLC system consisted of an autosampler (SIC Model 23, Tokyo, Japan), a variable-wavelength UV–visible detector (Soma, Tokyo, Japan) and a chromatographic pump (Waters Model 510). Separation was achieved on a reversed-phase Nucleosil 5C8 column (250 × 4 mm i.d., particle size 5 μm) (Macherey–Nagel, Duren, Germany). The mobile phase was acetonitrile–water–diethylamine (50:50:0.1, v/v/v) (pH 3.0, adjusted with orthophosphoric acid), and the flow rate was 1.0 ml min^{-1}. Osthole was monitored at 323 nm throughout the experiments. The system was operated at room temperature (25°C).

2.3. Animals

Male Sprague–Dawley rats (250–300 g) were obtained from the Laboratory Animal Center at the National Yang-Ming University. These animals were specifically pathogen free and kept in environmentally controlled quarters (temperature maintained at 24 ± 1°C and with a 12:12 h light–dark cycle) for at least 1 week before use. Standard laboratory chow and water were available at all times, except that the food was withdrawn 18 h prior to experiment.

2.4. Blood sampling

Rats were anesthetized with intraperitoneal urethane (0.8 g kg^{-1}). Additional dosages of 0.08 g kg^{-1} urethane were given if the rat showed signs of wakening during the experimental period. Blood samples (0.3 ml) were collected via cardiac puncture [8, 9] at times 2.5, 5, 10, 15, 20, 30, 45, 60, 90, 120 and 180 min after intravenous (i.v.) administration of osthole (10 mg kg^{-1}). Six rats were used for the experiment. Data from these samples were used to construct pharmacokinetic profiles by plotting the concentration of osthole in plasma vs. time.

2.5. Treatment of plasma samples

Each collected blood sample was transferred to a heparinized microcentrifuge tube and centrifuged at 8000*g* for 3 min (Eppendorf Model 5402, Germany). The resulting plasma (0.1 ml) was then mixed with 0.2 ml of acetonitrile containing paeonol (2 μg ml^{-1}) as an internal standard. The denatured protein precipitate was separated by centrifugation at 8000*g* for 3 min

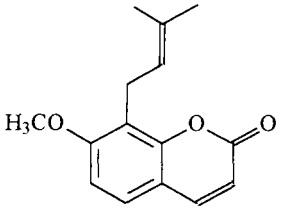

Fig. 1. Structure of osthole.

and a 20 μl aliquot of the supernatant was injected directly into the HPLC system. The same sample handing process was used for recovery and precision determinations.

2.6. Recovery

Plasma samples were spiked with osthole at concentrations ranging from 0.5 to 2 μg ml^{-1}. The resulting peak-area ratios (osthole to internal standard) were compared with those of standards prepared in acetonitrile.

2.7. Precision

The precision over the entire working dose range was determined by replicate analyses of plasma samples ($n = 4$) spiked with three different concentrations (0.1, 0.5 or 2 μg ml^{-1}) of osthole. To determine the intra-assay variance, quadruplicate assays were carried out on the same samples at different times during the day. The inter-assay variance was determined by assaying the spiked samples in quadruplicate on days 1, 2, 4 and 6 after spiking. Relative standard deviations (RSDs) were calculated from these values.

2.8. Pharmacokinetic analysis

A calibration curve was constructed based on the determination by HPLC of various concentrations of osthole spiked in rat plasma. The concentration of osthole in rat plasma after i.v. administration was determined from the peak area by using the equation for linear regression from the calibration curve. All data were subsequently processed by the computer program PCNONLIN (SCI Software, Lexington, KY). The data for the area under the curve of concentration in plasma versus time (AUC_{0-inf}) were calculated by the trapezoidal method and extrapolated to infinite time.

3. Results

Under the conditions described above, the retention times of osthole and paeonol (internal standard) were found to be 11.49 and 5.62 min, respectively (Fig. 2A). The main characteristic spectral data obtained in the mobile phase showed absorption maxima at 203, 257 and 323 nm for osthole and at 214, 277 and 313 nm for paeonol (Fig. 2B).

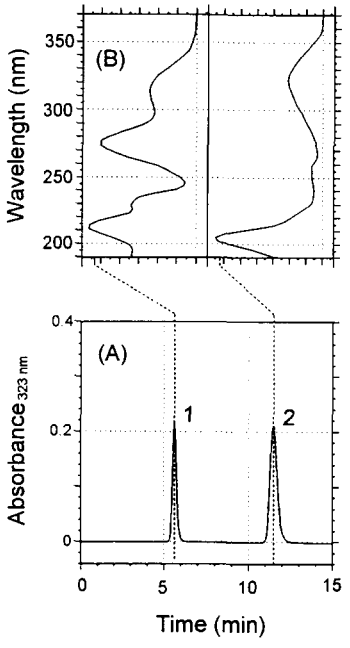

Fig. 2. (A) Chromatogram and (B) UV spectra of authentic osthole and paeonol (internal standard), measured with a photodiode-array detector (Waters Model 990). Peaks: 1 = paeonol; 2 = osthole.

The recoveries of osthole from rat plasma were found to be 95.49, 94.41 and 96.21% for concentrations 0.5, 1 and 2 μg ml^{-1}, respectively. The reproducibility of the method was also defined by examining both intra- and inter-assay variabilities. The intra-assay RSDs for osthole at concentrations of 0.5, 1 and 2 μg ml^{-1} were 8.89, 6.55 and 4.39%, respectively, and the inter-assay RSDs for osthole at the same concentrations were 8.09, 5.37 and 3.61%, respectively.

To determine the linearity and the detection limit of the HPLC method, rat plasma samples spiked with with six different concentrations of osthole (0.1–10 μg ml^{-1}) were analyzed.

The limits of the lowest concentration on the calibration curve can be measured with acceptable

accuracy (RSD < 20%). The lower practical limit of quantification was 0.1 μg ml^{-1}. With the procedure described above, the detection limit for osthole, at a signal-to-noise ratio of 3, was 0.05 μg ml^{-1} in rat plasma.

Fig. 3A shows the chromatogram of blank rat plasma. No discernible peaks were observed within the time frame in which osthole and paeonol were detected. Fig. 3B shows the chromatogram of rat plasma spiked with osthole (1 μg ml^{-1}) and internal standard. Fig. 3C shows the chromatogram of an osthole (0.79 μg ml^{-1}) sample obtained 20 min after i.v. administration of osthole (10 mg kg^{-1}) to a rat.

The data from the dose (Fig. 4) were found to fit best a two-compartment open model by the computer program PCNONLIN. The following equation applies to a two-compartment pharmacokinetic model:

$$C = A\,e^{-\alpha t} + B\,e^{-\beta t} \quad (1)$$

where A and B are the concentration (C) intercepts for fast and slow disposition phases, respectively, and α and β are disposition rate constants for fast and slow disposition phases, respectively. K_{12} and K_{21} are micro rate constants between the central and peripheral compartments and K_{10} is

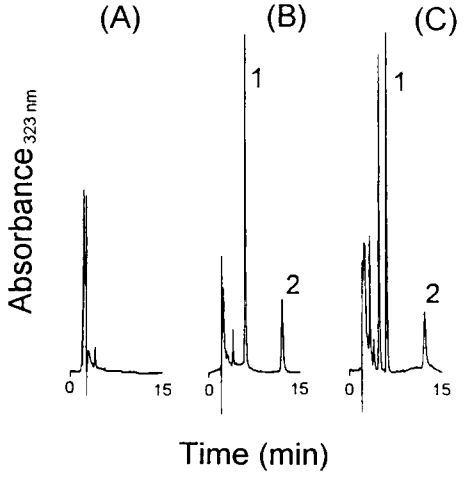

Fig. 3. Chromatograms of osthole in rat plasma: (A) blank plasma; (B) spike osthole (1 μg ml^{-1}) and paeonol (internal standard); (C) plasma sample 20 min after a 10 mg kg^{-1} i.v. administration of osthole (0.79 μg ml^{-1}). Peaks: 1 = paeonol; 2 = osthole.

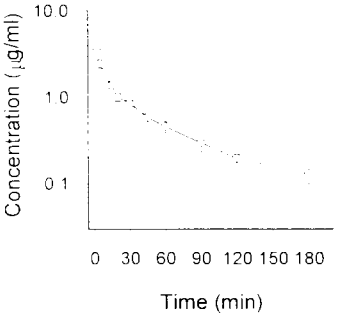

Fig. 4. Plasma concentration–time curve after i.v. administration of osthole in rats at doses of 10 mm kg^{-1}.

the elimination rate constant. The distribution half-life ($t_{1/2,\alpha}$) and elimination half-life ($t_{1/2,\beta}$) of osthole as shown in the initial phase and terminal phase of the plasma concentration–time curve were determined as $0.693/\alpha$ and $0.693/\beta$, respectively. The pharmacokinetic parameters, as derived from these data and calculated by PCNONLIN, are shown in Table 1.

4. Discussion

The complementary use of photodiode-array detection for identifying an analyte compound by its retention time and UV spectrum is more reliable than a UV detector, which gives only the retention time [8–11]. Photodiode-array detection allowed the observation of the full UV spectrum of each peak as it eluted from the chromatographic column. Hence the detection of other components could be observed.

From the UV spectra and the retention time of paeonol (internal standard), osthole (Fig. 2) was identified. The unidentified peaks (retention times 3.1 and 4.5 min) in Fig. 3C may be metabolites of osthole, which appear in plasma after i.v. administration of osthole. However, the identity of the unknown compounds remains to be evaluated.

A statistical non-linear regression program was accessed through the JANA and PCNONLIN programs for kinetic analysis. The pharmacokinetic models (one- vs. two-compartment) were compared according to Akaike's information criterion (AIC) [12] and the Schwarz criterion (SC) [13], and minimum AIC and SC values were

Table 1
Pharmacokinetic parameters of osthole in rats after 10 mg kg^{-1} i.v. administration

Parameter[a]	Estimate
A ($\mu g\ ml^{-1}$)	3.47 ± 0.36
B ($\mu g\ ml^{-1}$)	1.37 ± 0.12
α (min^{-1})	0.21 ± 0.048
β (min^{-1})	0.018 ± 0.002
K_{10} (min^{-1})	0.065 ± 0.015
K_{12} (min^{-1})	0.18 ± 0.084
K_{21} (min^{-1})	0.083 ± 0.022
Vol ($l\ kg^{-1}$)	1.97 ± 0.29
$t_{1/2,\alpha}$ (min)	3.59 ± 0.81
$t_{1/2,\beta}$ (min)	41.13 ± 5.73
Cl ($l\ kg^{-1}\ min^{-1}$)	0.11 ± 0.014
AUC ($\mu g\ min\ ml^{-1}$)	99.39 ± 12.47
AUMC ($\mu g\ min^2\ ml^{-1}$)	5162 ± 1337
MRT (min)	48.41 ± 6.20
V_{ss}, ($l\ kg^{-1}$)	4.93 ± 0.28

Data are expressed as mean ± SEM.
[a] Cl = clearance; Vol = central volume of distribution; V_{ss} = volume of distribution at steady state. See text for other abbreviations.

regarded as the best representation of the plasma concentration–time course data. A two-compartment open model with elimiation from the central compartment was proposed and validated through the program to explain the apparent biphasic disposition of osthole in rat plasma after i.v. administration.

The non-compartmental method for calculating the disposition parameters of osthole is based on the theory of statistical moments [14]. The area under the concentration curve of a plot of the product of concentration and time versus time from zero time to infinity is often referred to as the area under the moment curve (AUMC) [14]. The ratio of AUMC to AUC for osthole is a measure of its mean residence time (MRT) [15]. The MRT calculated after i.v. administration is the statistical moment analogy to drug elimination half-life. After administration of the osthole (10 mg kg^{-1}, i.v.), MRT and $t_{1/2,\beta}$ were 48.41 and 41.13 min, respectively (Table 1). Like the half-life, MRT is a function of both distribution and elimination. Whereas, the half-life indicates the time required to eliminate 50% of the dose, MRT_{iv} represents the time required to eliminate 63.2% of the dose.

In conclusion, the present method allows high selectivity and reliability and the relative simplicity permits its use for pharmacokinetic studies. Analysis of data after i.v. injection of osthole at 10 mg kg^{-1} yields a two-compartment pharmacokinetic model.

Acknowledgement

This study was supported by research grant NSC-85-2331-B-077-004 from the National Science Council, Taiwan, to T.H.T.

References

[1] Jengsu New Medical College, Dictionary of Chinese Medicine. Shanghai Scientific and Technological Publisher, Shanghai, 1984, p. 1703.
[2] H.M. Chang and P.H. But, Pharmacology and Application of Chinese Materia Medica, Vol. II, World Scientific Publishing, Singapore, 1989, pp. 896–899.
[3] Y.F. Chen, H.Y. Tsai and T.S. Wu, Planta Med., 61 (1995) 2–8.
[4] T.S. Wu, M.J. Liou, F.N. Ko and C.M. Teng, Chin. Pharm. J., 42 (1990) 317–322.
[5] F.N. Ko, T.S. Wu, M.J. Liou, T.F. Huang and C. M. Teng, Thromb. Haemost., 62 (1989), 996–999.
[6] F.N. Ko, T.S. Wu, M.J. Liou, T.F. Huang and C.M. Teng, Eur. J. Pharmacol., 219 (1992) 29–34.
[7] C.M. Teng, C.H. Lin, F.N. Ko, T.S. Wu and T.F. Huang, Naunyn-Schmiedeberg's Arch Pharmacol., 349 (1994) 202–208.
[8] T.H. Tsai, C.J. Chou and C.F. Chen, J. Pharm. Sci., 83 (1994) 1307–1309.
[9] T.H. Tsai, C.J. Chou, F.C. Cheng and C.F. Chen, J. Chromatogr. B., 655 (1994) 41–45.
[10] T.H. Tasi, C.M. Chen and C.F. Chen, J. Pharm. Pharmacol., 44 (1992) 620–623.
[11] T.H. Tsai, C.J. Chou and C.F. Chen, Drug Metab. Dispos., 22 (1994) 518–521.
[12] K. Yamoaka, T. Nakagawa and T. Uno, J. Pharmacokinet. Biopharm., 6 (1978) 165–175.
[13] G. Schwarz, Ann. Stat., 6 (1978) 461–464.
[14] M. Gibaldi and D. Perrier, Pharmacokinetics, Marcel Dekker, New York, 1982, pp. 409–417.
[15] L.Z. Benet and R.L. Galeazzi, J. Pharm. Sci., 68 (1979) 1071–1074.